Cell Reports, Volume *40*

Supplemental information

Engineering of immune checkpoints B7-H3 and CD155 enhances immune compatibility of MHC-I$^{-/-}$ iPSCs for β cell replacement

Raniero Chimienti, Tania Baccega, Silvia Torchio, Fabio Manenti, Silvia Pellegrini, Alessandro Cospito, Angelo Amabile, Marta Tiffany Lombardo, Paolo Monti, Valeria Sordi, Angelo Lombardo, Mauro Malnati, and Lorenzo Piemonti

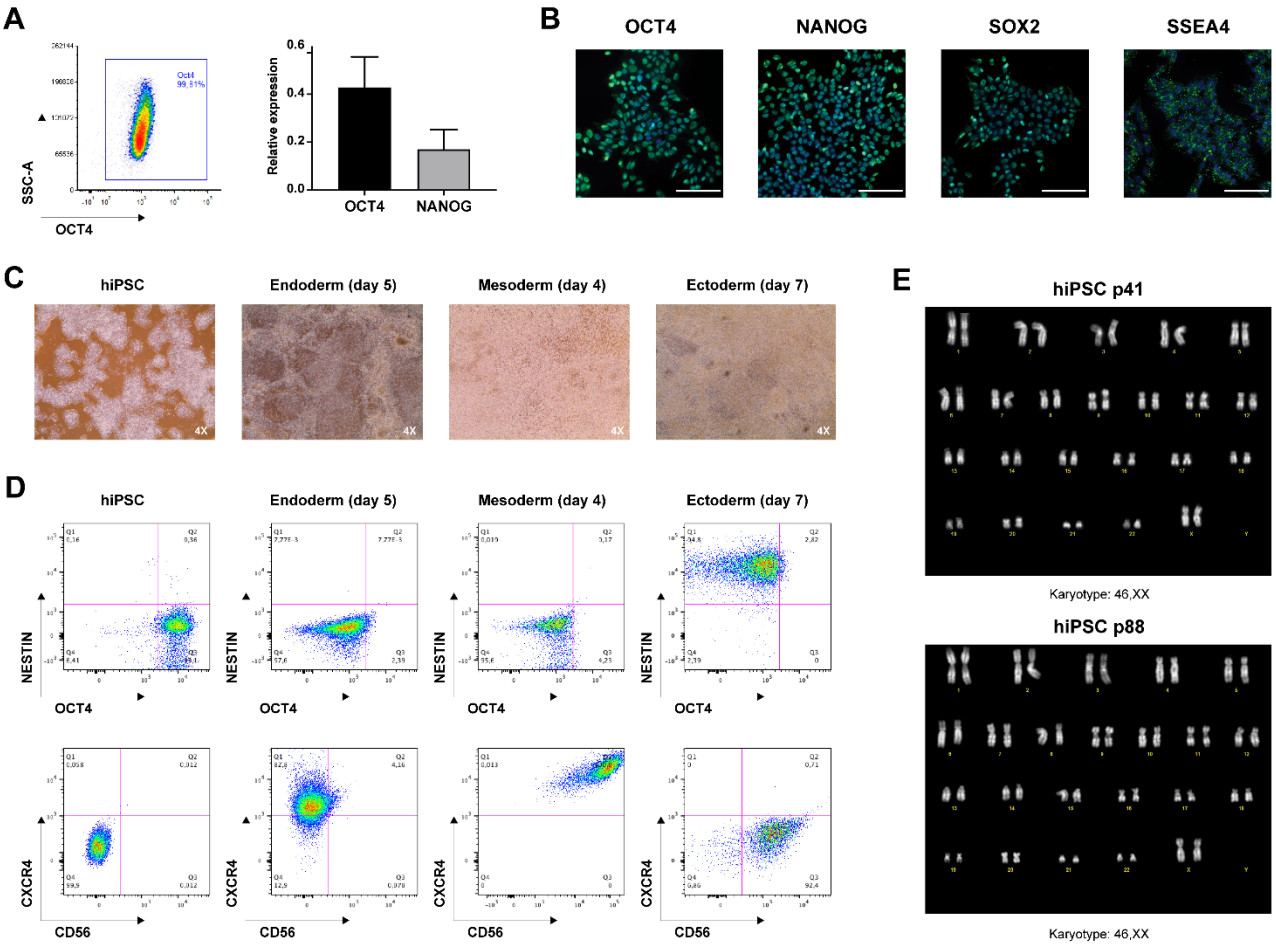
A
Oct4
99,81%
SSC-A
OCT4
Relative expression
0.6
0.4
0.2
0.0
OCT4
NANOG
B
OCT4
NANOG
SOX2
SSEA4
C
hiPSC
Endoderm (day 5)
Mesoderm (day 4)
Ectoderm (day 7)
4X
D
hiPSC
Endoderm (day 5)
Mesoderm (day 4)
Ectoderm (day 7)
NESTIN
OCT4
CXCR4
CD56
E
hiPSC p41
Karyotype: 46,XX
hiPSC p88
Karyotype: 46,XX
F
Endoderm markers
Mesoderm markers
Ectoderm markers
FC over undifferentiated control (log scale)
iPSC
Endoderm
Mesoderm
Ectoderm
hiPSC-derived endoderm (algorithm score)
Endoderm 0,80
Mesoderm -0,74
Ectoderm 0,00
hiPSC-derived mesoderm (algorithm score)
Endoderm -0,61
Mesoderm 1,97
Ectoderm -1,51
hiPSC-derived ectoderm (algorithm score)
Endoderm -0,97
Mesoderm -0,51
Ectoderm 0,79

Figure S1. Human iPSCs express pluripotency markers and preserve their capability to differentiate *in vitro* into three germ layers. Related to Figure 1 and 2 (A) Pluripotency marker expression by flow cytometry (OCT4) and qRT-PCR (OCT4 and NANOG) into wild type iPSCs. GAPDH was used as normalizer gene. Error bars represent standard deviation. N = 3 independent experiments. Each experiment used the same cell line (CGTRCiB10) at different passages and state of confluence. **(B)** Immunofluorescence staining on wild type iPSCs for pluripotency markers OCT4, NANOG, SOX2 and SSEA4 (all in green). Cell nuclei are stained with Hoechst (blue). Scale bar 100 µm (20x magnification). **(C)** Phase contrast microscope view showing the morphology of iPSCs, and three germ layers obtained by using Trilineage Differentiation Kit. **(D)** Pluripotent, endoderm, mesoderm and ectoderm marker expression patterns assayed by flow cytometry. Gates were set by referring to scatter plot of related unstained or isotype controls. **(E)** Conventional staining of the metaphase I for karyotype analysis of iPSCs at passages 41 and 88, after treatment for 16 hours with 0.2 µg/ml Colchicine. **(F)** Relative mRNA expression of trilineage specific genes into iPSCs and iPSC-derived three germ layers. ACTB, EP300 and SMAD1 were used as normalizer genes. Data are plotted on the logarithmic scale as fold change over unrelated undifferentiated control. At the bottom-right of panel, algorithm scores for the samples showing up- or down-regulation of the endoderm, mesoderm or ectoderm markers relative to the reference set of nine undifferentiated pluripotent stem cell lines.

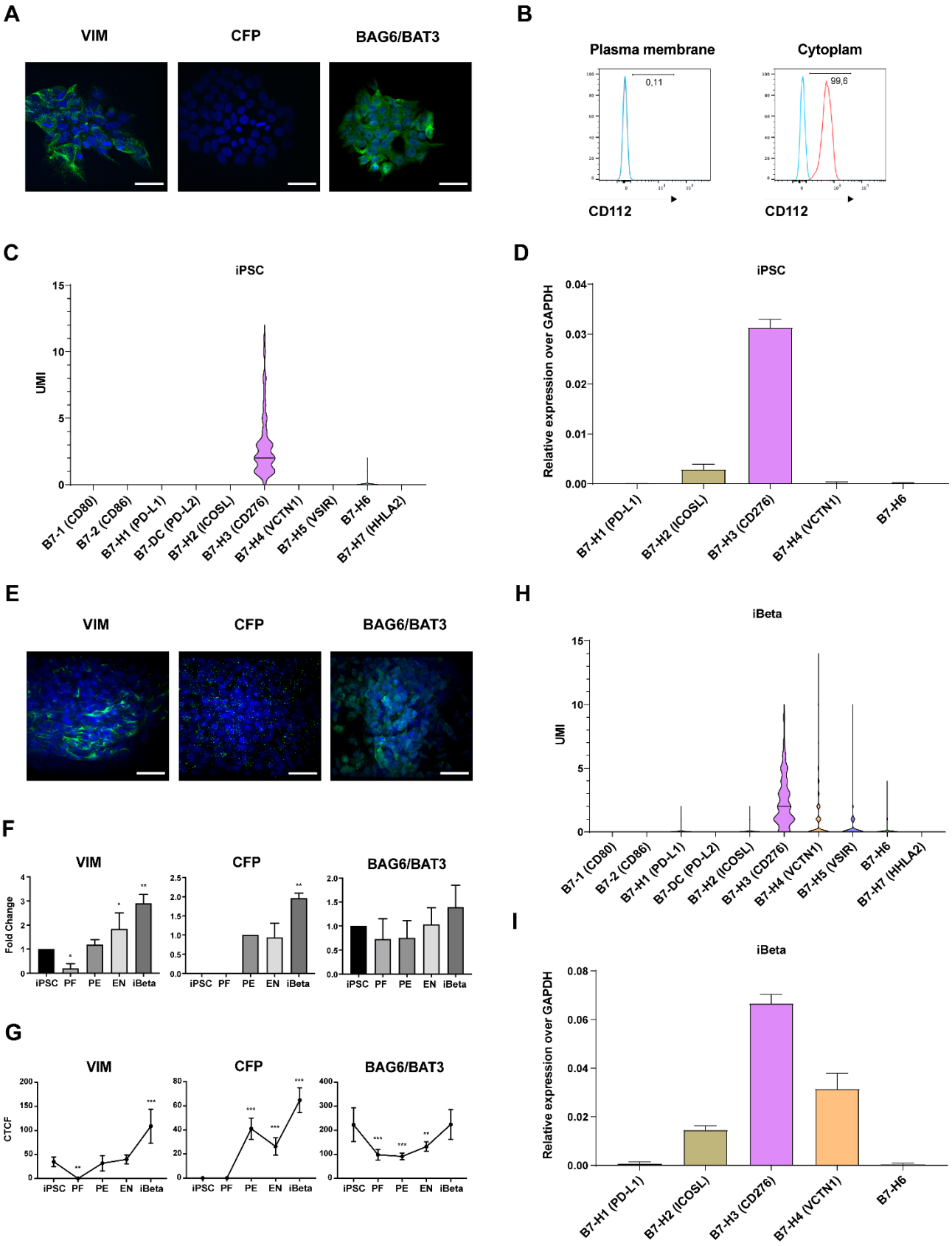
A
VIM
CFP
BAG6/BAT3
B
Plasma membrane
Cytoplam
0,11
99,6
CD112
CD112
C
iPSC
UMI
B7-1 (CD80)
B7-2 (CD86)
B7-H1 (PD-L1)
B7-DC (PD-L2)
B7-H2 (ICOSL)
B7-H3 (CD276)
B7-H4 (VCTN1)
B7-H5 (VSIR)
B7-H6
B7-H7 (HHLA2)
D
iPSC
Relative expression over GAPDH
B7-H1 (PD-L1)
B7-H2 (ICOSL)
B7-H3 (CD276)
B7-H4 (VCTN1)
B7-H6
E
VIM
CFP
BAG6/BAT3
F
VIM
CFP
BAG6/BAT3
Fold Change
iPSC PF PE EN iBeta
G
VIM
CFP
BAG6/BAT3
CTCF
iPSC PF PE EN iBeta
H
iBeta
UMI
B7-1 (CD80)
B7-2 (CD86)
B7-H1 (PD-L1)
B7-DC (PD-L2)
B7-H2 (ICOSL)
B7-H3 (CD276)
B7-H4 (VCTN1)
B7-H5 (VSIR)
B7-H6
B7-H7 (HHLA2)
I
iBeta
Relative expression over GAPDH
B7-H1 (PD-L1)
B7-H2 (ICOSL)
B7-H3 (CD276)
B7-H4 (VCTN1)
B7-H6

Figure S2. Expression pattern of intracellular NK activating ligands and B7 family genes on undifferentiated iPSCs and during *in vitro* differentiation into pancreatic β cells. Related to Figure 2 (A) Immunofluorescence staining for intracellular NK ligands vimentin (VIM), properdin (CFP) or BAG6/BAT3 (green). Cell nuclei were counterstained with Hoechst (blue). Scale bar 40 um (40X magnification) **(B)** Representative histograms of iPSCs after extracellular or intracellular staining with anti-CD112 mAb (red), using isotype Ab as staining control (light blue). **(C)** Violin plots of the normalized log-expression values calculated as Unique Molecular Identifier (UMI) of B7 family genes in the undifferentiated iPSC dataset. **(D)** Relative expression by qRT-PCR (mean ± SD; n = 3 independent experiments using batches of the same cell line at different passages) of *B7-H1*, *-H2*, *-H3*, *-H4* and *-H6* genes in undifferentiated iPSCs. *GAPDH* was used as normalizer gene. **(E)** Immunofluorescence staining on terminally differentiated cells (iBeta) for intracellular NK ligands VIM, CFP or BAG6/BAT3, followed by incubation with Alexa Fluor 488-conjugated secondary antibody (green). Cell nuclei were counterstained with Hoechst (blue). Scale bar 40 um (40X magnification). **(F)** Relative mRNA expression (mean ± SD; n = 3 independent *in vitro* differentiations) of NK ligand VIM, CFP or BAG6/BAT3 during pancreatic differentiation as assayed by qRT-PCR. GAPDH was used as normalizer gene. Data are reported as fold change over undifferentiated cells. **(G)** Average corrected total cell fluorescence (CTCF) of intracellular NK ligand VIM, CFP or BAG6/BAT3 positive cells in iPSCs and during pancreatic differentiation. Error bars represent standard deviation. N = 5 independent experiments. **(H)** Violin plots of the normalized log-expression values calculated as Unique Molecular Identifier (UMI) of B7 family genes in the iBeta dataset. **(I)** Relative expression by qRT-PCR (mean ± SD; n = 3 independent *in vitro* differentiations) of *B7-H1*, *-H2*, *-H3*, *-H4* and *-H6* genes in pancreatic terminally differentiated iPSCs. *GAPDH* was used as normalizer gene. Each experiment involving only undifferentiated iPSCs utilized the same cell line (CGTRCiB10) at different passages and state of confluence. Each experiment involving differentiated cells was carried out performing different independent *in vitro* differentiations of the same iPSC clone (CGTRCiB10) at different passages. iPSC = undifferentiated iPSC; PF = posterior foregut; PE = pancreatic endoderm; EN = endocrine cells; iBeta = iPSC-β cells. Statistical significances were obtained with two-tailed t-test and are referred to comparison with the iPSC stage. * $p < 0.05$; ** $p < 0.01$; *** $p < 0.001$.

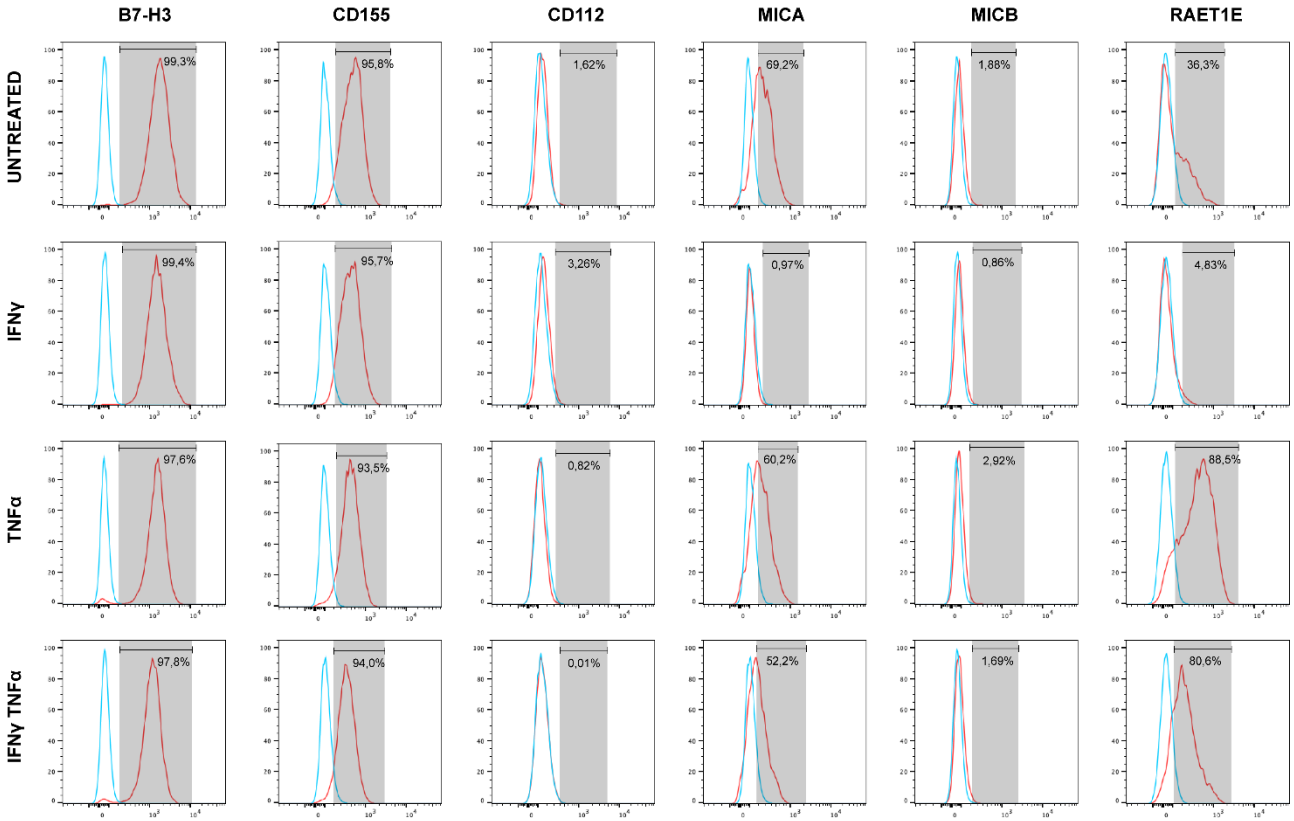

Figure S3. Exposure of iPSC to IFN-γ and/or TNF-α caused slight changes in the expression of NK activating ligands. Related to Figure 2. Representative histograms of staining with mAbs (red) for B7-H3, DNAM-1 ligands CD155 and CD112, NKG2D ligands MICA, MICB and RAET1E, or with related istotype control (light blue). Staining was performed on untreated iPSCs or iPSCs treated overnight with 10 ng/ml IFN-γ, 50 ng/ml TNF-α or both (10 ng/ml IFN-γ and 50 ng/ml TNF-α).

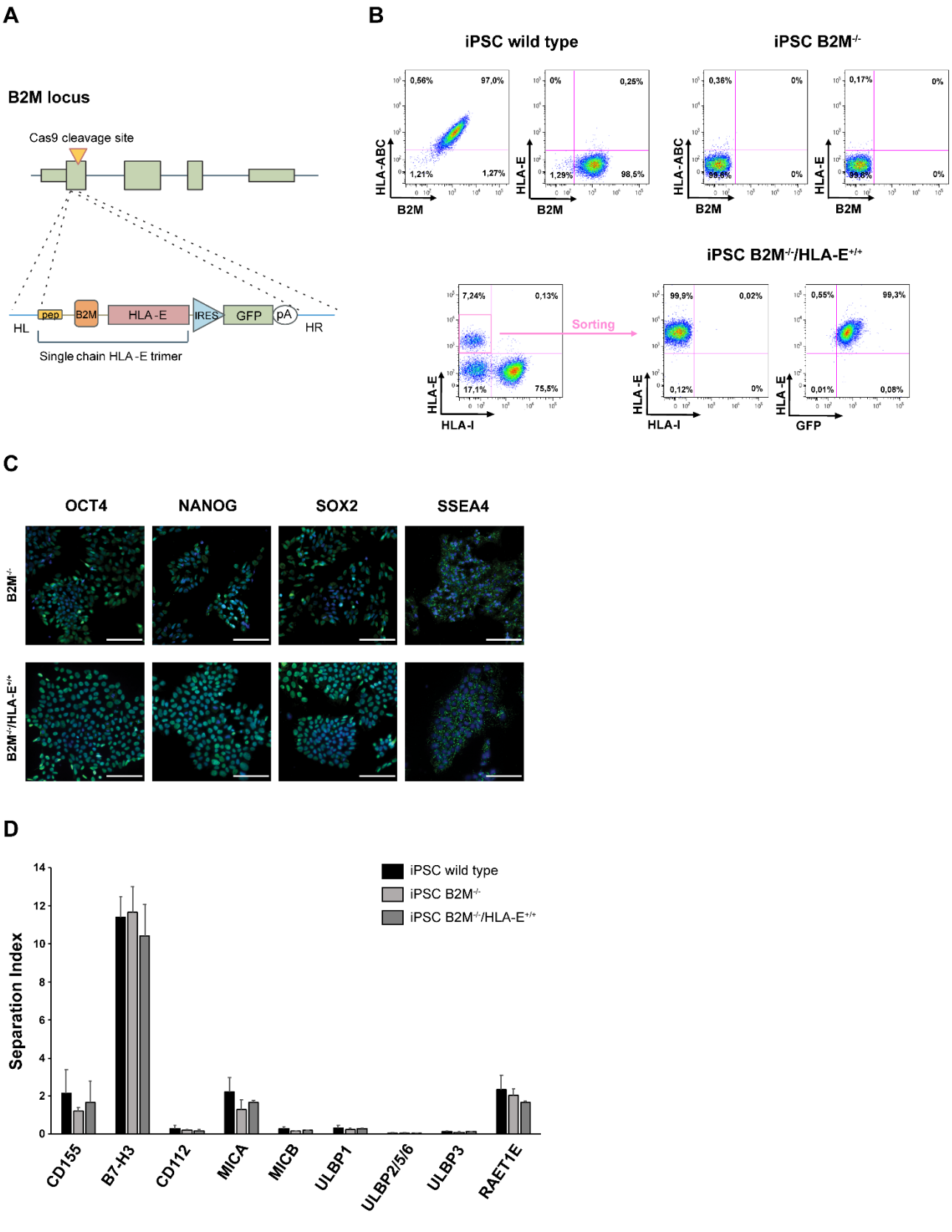
A
B2M locus
Cas9 cleavage site
pep
B2M
HLA-E
IRES
GFP
pA
HL
HR
Single chain HLA-E trimer
B
iPSC wild type
iPSC B2M-/-
iPSC B2M-/-/HLA-E+/+
HLA-ABC
HLA-E
B2M
HLA-I
GFP
Sorting
0,56%
97,0%
1,21%
1,27%
0%
0,25%
1,29%
98,5%
0,36%
0,17%
99,6%
7,24%
0,13%
17,1%
75,5%
99,9%
0,02%
0,12%
0,55%
99,3%
0,01%
0,08%
C
OCT4
NANOG
SOX2
SSEA4
B2M-/-
B2M-/-/HLA-E+/+
D
Separation Index
iPSC wild type
iPSC B2M-/-
iPSC B2M-/-/HLA-E+/+
CD155
B7-H3
CD112
MICA
MICB
ULBP1
ULBP2/5/6
ULBP3
RAET1E

Figure S4. Gene engineered B2M$^{-/-}$ and B2M$^{-/-}$/HLA-E$^{+/+}$ iPSCs remain undifferentiated and maintain unaltered the expression pattern of NK activating ligands. Related to Figure 3, 4, 5, 6 and 7 (A) Schematic representation of the *B2M* locus, indicating cutting site (yellow triangle) of the CRISPR/Cas9 complex. HLA-E-containing construct knocked into *B2M* locus is also showed. GFP was used as reporter gene. HR/HL = right/left homology arms; pep = peptide; pA = polyadenylation signal. **(B)** FACS plots for pan class I MHC molecules, B2M and HLA-E proteins on wild type, B2M$^{-/-}$ and B2M$^{-/-}$/HLA-E$^{+/+}$ iPSCs. Knocked-in cells with HLA-E-IRES-GFP construct were enriched by cell sorting and assayed for HLA-E and GFP expression. Gates were set by referring to scatter plot of related unstained or isotype controls. **(C)** Immunofluorescence staining on B2M$^{-/-}$ and B2M$^{-/-}$/HLA-E$^{+/+}$ iPSC lines for pluripotency markers OCT4, NANOG, SOX2 and SSEA4 (green). Cell nuclei are stained with Hoechst (blue). Scale bar 100 μm (20x magnification). **(D)** Comparison by qRT-PCR of expression profile of the NK activating ligands between wild type and gene engineered B2M$^{-/-}$ and B2M$^{-/-}$ /HLA-E$^{+/+}$ iPSCs. *GAPDH* was used as normalizer gene. Error bars represent standard deviation. N = 3. Each experiment was performed by using the same cell line at different passages and state of confluence. One-way ANOVA followed by Tukey's post hoc test was performed.

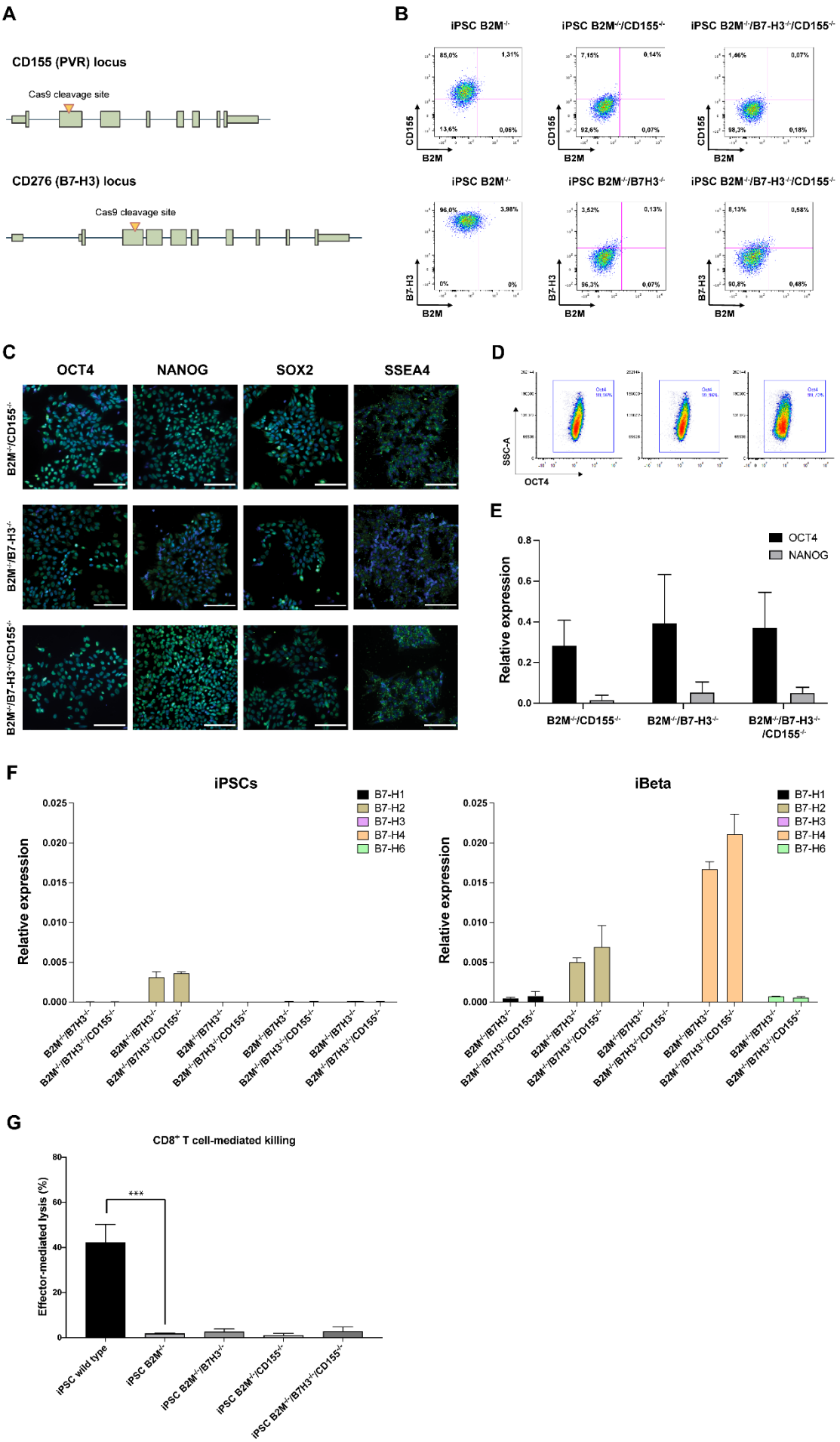
A
CD155 (PVR) locus
Cas9 cleavage site
CD276 (B7-H3) locus
Cas9 cleavage site
B
iPSC B2M-/-
iPSC B2M-/-/CD155-/-
iPSC B2M-/-/B7-H3-/-/CD155-/-
iPSC B2M-/-
iPSC B2M-/-/B7H3-/-
iPSC B2M-/-/B7-H3-/-/CD155-/-
CD155
B7-H3
B2M
C
OCT4
NANOG
SOX2
SSEA4
B2M-/-/CD155-/-
B2M-/-/B7-H3-/-
B2M-/-/B7-H3-/-/CD155-/-
D
SSC-A
OCT4
E
OCT4
NANOG
Relative expression
B2M-/-/CD155-/-
B2M-/-/B7-H3-/-
B2M-/-/B7-H3-/-/CD155-/-
F
iPSCs
iBeta
B7-H1
B7-H2
B7-H3
B7-H4
B7-H6
Relative expression
G
CD8+ T cell-mediated killing
Effector-mediated lysis (%)
***
iPSC wild type
iPSC B2M-/-
iPSC B2M-/-/B7H3-/-
iPSC B2M-/-/CD155-/-
iPSC B2M-/-/B7H3-/-/CD155-/-

Figure S5. Gene edited B2M$^{-/-}$/B7-H3$^{-/-}$, B2M$^{-/-}$/CD155$^{-/-}$ and B2M$^{-/-}$/B7-H3$^{-/-}$/CD155$^{-/-}$ iPSCs preserve pluripotency, while specific knock-out of B7-H3 does not affects expression of other B7 family genes. Related to Figure 4, 5, 6 and 7 (A) Schematic representations of the PVR and B7-H3 loci, indicating cutting site (yellow triangle) of CRISPR/Cas9 complex. **(B)** FACS plots for B2M and CD155 or B7-H3 proteins on purified iPSC clones knocked-out for CD155 and/or B7-H3. **(C)** Immunofluorescence staining on B2M$^{-/-}$/B7-H3$^{-/-}$, B2M$^{-/-}$/CD155$^{-/-}$ and B2M$^{-/-}$/B7-H3$^{-/-}$/CD155$^{-/-}$ iPSC lines for pluripotency markers OCT4, NANOG, SOX2 and SSEA4 (all in green). Cell nuclei are stained with Hoechst (blue). Scale bar 100 μm (20x magnification). **(D)** Pluripotency marker expression by flow cytometry (OCT4) and **€** qRT-PCR (*OCT4* and *NANOG*) into B2M$^{-/-}$/B7-H3$^{-/-}$, B2M$^{-/-}$/CD155$^{-/-}$ and B2M$^{-/-}$/B7-H3$^{-/-}$/CD155$^{-/-}$ iPSCs. *GAPDH* was used as normalizer gene. Error bars represent standard deviation. N = 3 independent experiments. **(F)** Relative expression by qRT-PCR of *B7-H1*, *-H2*, *-H3*, *-H4* and *-H6* genes in both undifferentiated (iPSCs) and terminally differentiated (iBeta) B2M$^{-/-}$/B7-H3$^{-/-}$ and B2M$^{-/-}$/B7-H3$^{-/-}$/CD155$^{-/-}$ cell lines. *GAPDH* was used as normalizer gene. Error bars represent standard deviation. N = 3 independent experiments. Each experiment used different independent *in vitro* differentiations of the edited cell lines at different passages. **(G)** Immune response of allogeneic CD8^{+} T cells against unedited and edited iPSCs measured by cytotoxicity assay at 1:5 target:effector ratio. N = 3 independent experiments. Each experiment was performed by using CD8^{+} T cells against the same cell line at different passages. One-way ANOVA followed by Dunnett's post hoc test was performed using B2M$^{-/-}$ as control.

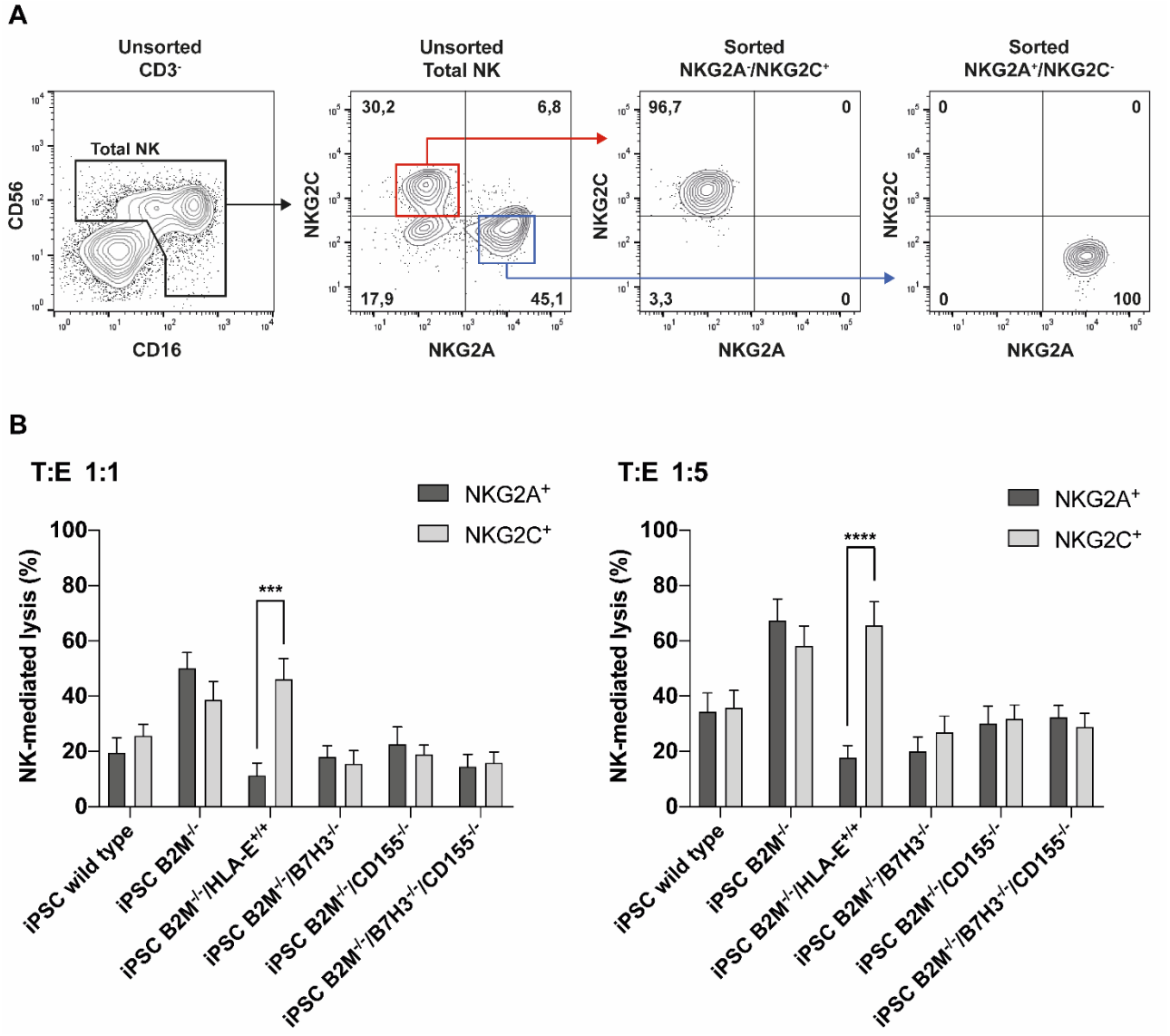
A
Unsorted
CD3-
Total NK
CD56
CD16
Unsorted
Total NK
30,2
6,8
17,9
45,1
NKG2C
NKG2A
Sorted
NKG2A-/NKG2C+
96,7
0
3,3
0
Sorted
NKG2A+/NKG2C-
0
0
0
100
B
T:E 1:1
T:E 1:5
NKG2A+
NKG2C+
NK-mediated lysis (%)
***
****
iPSC wild type
iPSC B2M-/-
iPSC B2M-/-/HLA-E+/+
iPSC B2M-/-/B7H3-/-
iPSC B2M-/-/CD155-/-
iPSC B2M-/-/B7H3-/-/CD155-/-

Figure S6. Activating ligand knock-out exerts protective effects against cytotoxic activity of NKG2C$^+$ subpopulations. Related to Figure 5. (A) Representative gating strategy illustrating the total NK cells sub-gated in the NKG2A$^+$ and NKG2C$^+$ subsets. On the right are reported the relative contour plots of sorted NKG2A$^+$/NKG2C$^-$ and NKG2A$^-$/NKG2C$^+$ NK cells used for cytotoxicity experiments. **(B)** Cytotoxicity on iPSC lines after co-incubation NKG2A$^+$ and NKG2C$^+$ NK cell subsets at the indicated target:effector ratio for 4 hours. Percentage of PI-positive target cells was measured by flow cytometry and data were normalized on basal cell death percentage occurring in target cells after incubation w/o effectors. Error bars indicate standard deviation. N = 6. All experiments were conducted using six different donors (one for each experiment). Each cytotoxicity experiment was carried out by using NKG2A$^+$ and NKG2C$^+$ cells derived from the same NK donor. One-way ANOVA followed by a Tukey's test was performed. * $p < 0.05$; ** $p < 0.01$; *** $p < 0.001$; **** $p < 0.0001$.

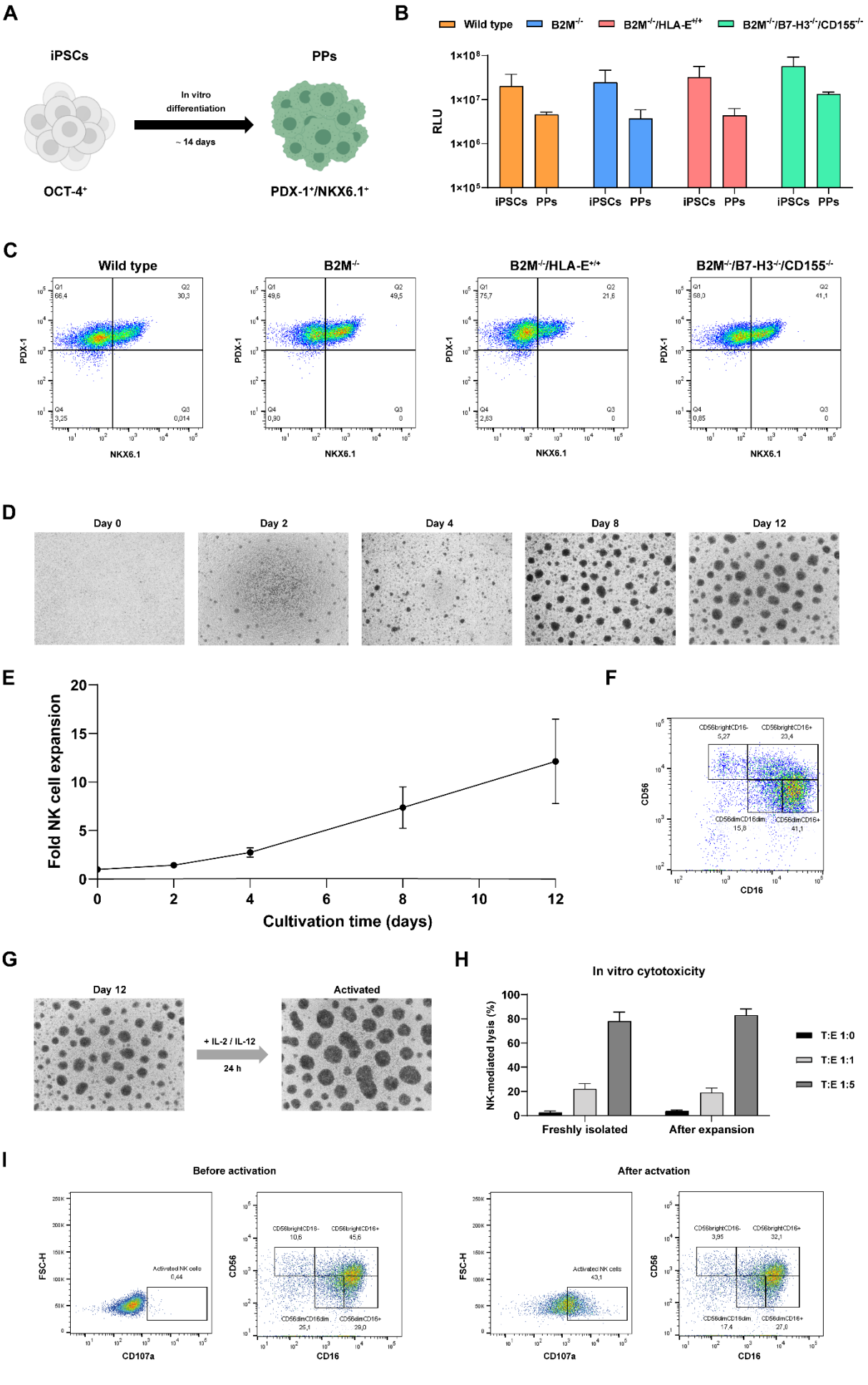
A
iPSCs
PPs
In vitro differentiation
~ 14 days
OCT-4+
PDX-1+/NKX6.1+
B
Wild type
B2M-/-
B2M-/-/HLA-E+/+
B2M-/-/B7-H3-/-/CD155-/-
RLU
1×10^8
1×10^7
1×10^6
1×10^5
iPSCs PPs iPSCs PPs iPSCs PPs iPSCs PPs
C
Wild type
B2M-/-
B2M-/-/HLA-E+/+
B2M-/-/B7-H3-/-/CD155-/-
PDX-1
NKX6.1
Q1 66,4
Q2 30,3
Q4 3,25
Q3 0,014
Q1 49,6
Q2 49,5
Q4 0,90
Q3 0
Q1 75,7
Q2 21,6
Q4 2,63
Q3 0
Q1 58,0
Q2 41,1
Q4 0,85
Q3 0
D
Day 0
Day 2
Day 4
Day 8
Day 12
E
Fold NK cell expansion
Cultivation time (days)
0
5
10
15
20
0
2
4
6
8
10
12
F
CD56
CD16
CD56brightCD16- 5,27
CD56brightCD16+ 23,4
CD56dimCD16dim 15,8
CD56dimCD16+ 41,1
G
Day 12
Activated
+ IL-2 / IL-12
24 h
H
In vitro cytotoxicity
NK-mediated lysis (%)
0
20
40
60
80
100
Freshly isolated
After expansion
T:E 1:0
T:E 1:1
T:E 1:5
I
Before activation
After actvation
FSC-H
CD107a
Activated NK cells 0,44
Activated NK cells 43,1
CD56
CD16
CD56brightCD16- 10,6
CD56brightCD16+ 45,6
CD56dimCD16dim 25,1
CD56dimCD16+ 29,0
CD56brightCD16- 3,95
CD56brightCD16+ 32,1
CD56dimCD16dim 17,4
CD56dimCD16+ 27,0

Figure S7. Characterization of luciferase-expressing iPSC lines differentiated into PPs and of *in vitro* expanded donor-derived primary NK cells. Related to Figure 7 (A) Cartoon of 14-days differentiation to pancreatic progenitors (PPs). Markers of pluripotency (OCT4) and pancreatic progenitors (PDX-1, NKX6.1) are reported. **(B)** Relative light units (RLU) of luciferase-expressing cell lines,before (iPSCs) and after (PPs) differentiation. **(C)** FACS plot for PP makers PDX-1 and NKX6.1 on Wild type and edited cell lines after 14-days differentiation. Gates were set by referring to scatter plot of related unstained controls. **(D)** Representative phase contrast microscope view showing allogeneic donor-derived primary NK cells after isolation (day 0) and during expansion protocol with IL-2/IL-15. (E) Growth curve of NK cells during expansion protocol. Error bars represent standard deviation. N = 12 experiments carried out using twelve distinct donors. **(F)** Representative FACS plot of staining for CD56 and CD16 of NK cells after 12 days in expansion medium. Gates highlight the NK subsets $CD56_{bright}/CD16^{-}$, $CD56_{bright}/CD16^{+}$, $CD56_{dim}/CD16_{dim}$ and $CD56_{dim}/CD16^{+}$. (G) Representative phase contrast microscope view showing NK cells at the end of 12-days *in vitro* expansion protocol (left) and after activation with IL-2/IL-12 (right). **(H)** Comparison between freshly isolated and expanded NK cells of their killing activity against K562 cells at different target:effector ratios. N = 6 experiments carried out using 6 different donor-derived NK cells. **(I)** Representative FACS plot of CD107a (degranulation maker), CD56 and CD16 expression of *in vitro* expanded NK cells before (left) and after (right) activation with IL-2/IL-12. Gates highlight the following NK subsets: $CD56_{bright}/CD16^{-}$, $CD56_{bright}/CD16^{+}$, $CD56_{dim}/CD16_{dim}$ and $CD56_{dim}/CD16^{+}$.